# Insula response and connectivity during social and non-social attention in children with autism

Paola Odriozola,[1,*] Lucina Q. Uddin,[2,3,*] Charles J. Lynch,[1] John Kochalka,[1] Tianwen Chen,[1] and Vinod Menon[1,4,5]

[1]Department of Psychiatry and Behavioral Sciences, Stanford University School of Medicine, Stanford, CA 94305, USA, [2]Department of Psychology, University of Miami, Coral Gables, FL 33124, USA, [3]Neuroscience Program, University of Miami Miller School of Medicine, Miami, FL 33136, USA, [4]Department of Neurology and Neurological Sciences, Stanford University School of Medicine, Stanford, CA 94305, USA, and [5]Stanford Neuroscience Institute, Stanford University School of Medicine, Stanford, CA 94305, USA

Correspondence should be addressed to Vinod Menon, Stanford University School of Medicine, 401 Quarry Rd., Stanford, CA 94305, USA.
E-mail: menon@stanford.edu

*These two authors contributed equally to this work.

## Abstract

Autism spectrum disorder (ASD) is characterized by reduced attention to salient social stimuli. Here, we use two visual oddball tasks to investigate brain systems engaged during attention to social (face) and non-social (scene) stimuli. We focused on the dorsal and ventral subdivisions of the anterior insula (dAI and vAI, respectively), anatomically distinct regions contributing to a 'salience network' that is known to regulate attention to behaviorally meaningful stimuli. Children with ASD performed comparably to their typically developing (TD) peers, but they engaged the right dAI and vAI differently in response to deviant faces compared with deviant scenes. Multivariate activation patterns in the dAI reliably discriminated between children with ASD and TD children with 85% classification accuracy, and children with ASD activated the vAI more than their TD peers. Children with ASD and their TD peers also differed in dAI connectivity patterns to deviant faces, with stronger within-salience network interactions in the ASD group and stronger cross-network interactions in the TD group. Our findings point to atypical patterns of right anterior insula activation and connectivity in ASD and suggest that multiple functions subserved by the insula, including attention and affective processing of salient social stimuli, are aberrant in children with the disorder.

Key words: salience network; oddball; autism spectrum disorder; functional connectivity; multivariate pattern analysis

## Introduction

One of the defining features of autism spectrum disorder (ASD) is reduced attention to social stimuli. In early childhood, signs of diminished interest in social stimuli, including the human face, are often noticed (Dawson *et al.*, 2004). These observations are catalogued in Kanner's initial report, where he writes of one child who 'paid no attention to persons around him' and of another who 'mostly ignored other people . . . when we had guests, he just would not pay any attention' (Kanner, 1943). The social motivation hypothesis of autism posits that children with ASD do not find social stimuli rewarding; as a consequence, these children are not motivated to engage with stimuli such as faces, thereby impairing the development of social skills (Dawson *et al.*, 2004; Scott-Van Zeeland *et al.*, 2010; Chevallier *et al.*, 2012). Despite ubiquitous reports of social attention deficits in ASD, very few studies have investigated cortical and subcortical systems underlying these attention processes in young children with the disorder.

A meta-analysis of neuroimaging studies in ASD has identified the anterior insula as an important locus of dysfunction in

tasks involving social cognition (Di Martino *et al.*, 2009a). Individuals with ASD were more likely to show hypoactivation of the right anterior insula in social compared with non-social processes across 39 studies. These findings led to the hypothesis that dysfunctional anterior insula activation and connectivity may play a prominent role in social deficits in ASD (Uddin and Menon, 2009). The anterior insula and anterior cingulate cortices together with subcortical limbic structures comprise the salience network (Seeley *et al.*, 2007), a system implicated in detecting and orienting attention to behaviorally meaningful stimuli (Menon and Uddin, 2010). This brain network integrates autonomic signals with information perceived from the external world to causally influence other large-scale brain networks including the central executive (CEN) and default mode networks (DMN) (Sridharan *et al.*, 2008; Menon and Uddin, 2010; Uddin *et al.*, 2011; Menon, 2015; Uddin, 2015). We hypothesized that atypical engagement of the salience network, specifically its anterior insula node, may contribute to diminished interest in social interaction in ASD (Chevallier *et al.*, 2012).

The 'oddball' task paradigm involves processing a sequence of events to detect a deviant stimulus embedded in a stream of repetitive standard stimuli (Crottaz-Herbette *et al.*, 2005). The task is typically used to index cognitive control and bottom-up attention (Downar *et al.*, 2000; Crottaz-Herbette and Menon, 2006; Chen *et al.*, 2015). Decades of functional neuroimaging studies have consistently shown that a network of brain regions including the anterior cingulate and anterior insular cortex is activated during the processing of deviant stimuli when compared with standard stimuli (Ardekani *et al.*, 2002; Crottaz-Herbette and Menon, 2006; Kim, 2014). The first neuroimaging study using face stimuli to investigate brain responses during the oddball task in adults with ASD demonstrated hyperactivation in insula and dorsal anterior cingulate regions during social deviant stimuli detection in the patient group (Dichter *et al.*, 2009). Another recent study of adults with ASD reported increased activation to social targets in the right insular cortex (Sabatino *et al.*, 2013).

To date, no studies have used the oddball paradigm to investigate social attention in young children with autism. Specifically, differences in brain responses to social and non-social stimuli have not been examined in children with ASD using this design, which probes both attention and cognitive control processes. In light of recent evidence for significant developmental differences in patterns of activation and connectivity in ASD (Dickstein *et al.*, 2013; Uddin *et al.*, 2013b; Nomi and Uddin, 2015a), it is becoming increasingly clear that results observed in adults with the disorder may not generalize to younger individuals.

Here, we address gaps in the literature by investigating social attention in autism using a brain network-based approach applied to data collected from school-age children, a younger age range than in previous investigations. We tested the hypothesis that social attention processes in children with ASD are characterized by differential response profiles and connectivity patterns in specific subdivisions of the insular cortex. Recent work has suggested that specific subdivisions of the insula are relatively specialized such that the ventral anterior insula (vAI) is more involved in affective and socio-emotional processing whereas the dorsal anterior insula (dAI) is involved in higher-level cognitive processes coordinating switches between large-scale brain networks (e.g. DMN and CEN) in response to salient stimuli (Sridharan *et al.*, 2008; Chang *et al.*, 2013; Uddin *et al.*, 2014a; Cai *et al.*, 2015; Menon, 2015; Uddin, 2015). Based on previous studies of social attention in adults

with ASD (Dichter *et al.*, 2009; Sabatino *et al.*, 2013), we therefore predicted that processing social stimuli (faces) but not non-social stimuli (scenes) would require greater attentional resources, and engage the dAI more in children with ASD.

## Materials and methods

### Participants

Participants were recruited in the San Francisco Bay Area through advertisements. Children with ASD were also recruited from the Stanford Autism Clinic and the Lucille Packard Children's Hospital. Children with a prior ASD diagnosis were evaluated using the Autism Diagnostic Interview-Revised (ADI-R; Lord *et al.*, 1994) and the Autism Diagnostic Observation Schedule-Second Edition (ADOS-2, module 3; Lord *et al.*, 2000; Gotham *et al.*, 2007) administered by a trained research assessor, and diagnoses were confirmed by a clinical psychologist. All participants were verbal and high-functioning, with relatively high intelligence quotient (IQ) scores as assessed using the Wechsler Abbreviated Scale of Intelligence (Wechsler, 1999; Table 1). All participants met the cutoff scores for autism using the diagnostic algorithm on the ADI-R and/or were in the autism spectrum range on the ADOS-2. A composite score, which includes scores for social interaction, communication, and restricted and repetitive behaviors was calculated for each: the ADI-R using the 'current' algorithm and the ADOS-2 (Gotham *et al.*, 2009; Hus and Lord, 2013). These scores served as a measure of severity of ASD symptoms. Participants gave written informed assent, and parents or guardians gave written informed consent. The study was approved by the Stanford University Institutional Review Board.

### Functional magnetic resonance imaging

Functional magnetic resonance imaging (fMRI) data were collected from 23 children with ASD and 22 age-matched typically developing (TD) children. Functional images were acquired on a 3T GE Signa scanner (General Electric, Milwaukee, WI) using a custom-built head coil. Head movement was minimized during scanning by small cushions. A total of 31 axial slices (4.0 mm thickness, 0.5 mm skip) parallel to the AC-PC line and covering the whole brain were imaged using a $T_2^*$-weighted gradient echo spiral in-out pulse sequence with the following parameters: TR = 2000 ms, TE = 30 ms, flip angle = 80°, 1 interleave, for the duration of a 4 min task scan.

A visual oddball detection task was used to assess brain responses to deviant stimuli. The oddball task is a simple paradigm that involves processing a sequence of events to detect a deviant stimulus embedded in a stream of repetitive standard stimuli. The task is designed to measure orienting of attention and reflects an individual's ability to monitor change in the environment and decide on a course of action (Crottaz-Herbette and Menon, 2006). For this study, social stimuli (faces) and non-social stimuli (outdoor scenes) were used.

All participants completed four runs (two face and two scene runs) of the oddball task, with each run lasting 4 min. The order of runs was counterbalanced across participants, as were the specific images used as 'standard' and 'deviant'. In each run, a total of 100 stimuli were presented for 400 ms each with a fixed inter-stimulus interval of 1750 ms. In 80% of the trials, the 'standard' stimulus was presented (i.e. a female individual with a neutral expression or an outdoor scene), in 20% of the trials, the 'deviant' stimulus was presented (i.e. a different female

**Table 1.** Participant demographics

| Measure | ASD (n = 20) | TD (n = 20) | P-value |
|---|---|---|---|
| Gender ratio | 18 M: 2 F | 16 M: 4 F | 0.38[a] |
| Age (years) | 10.51 ± 1.52 | 9.72 ± 1.61 | 0.12 |
| Handedness | 20 R | 19 R: 1 A | |
| FSIQ—WASI Scale | 110.20 ± 16.12 | 119.53 ± 15.18[b] | 0.07 |
| Diagnostic—ADI-R | | | |
|   Social interaction | 18.72 ± 6.53 | | |
|   Communication | 15.22 ± 5.09 | | |
|   Restricted and repetitive behaviors | 6.33 ± 2.50 | | |
|   Composite score | 32.61 ± 10.58 | | |
| Diagnostic—ADOS-2 | | | |
|   Total: social affect and restricted and repetitive behavior | 12.39 ± 3.79 | | |
|   Composite score | 7.22 ± 1.73 | | |

Demographic and mean full-scale IQ (FSIQ) scores are shown for the sample. M, Male; F, Female; R, Right handed; A, Ambidextrous; WASI, Wechsler Abbreviated Scale of Intelligence (Wechsler, 1999); ADI-R, Autism Diagnostic Interview- Revised; ADOS-2 (Lord et al., 1994), Autism Diagnostic Observation Schedule, Second Edition (Lord et al., 2000; Gotham et al., 2007). ADI-R scores use 'diagnostic' algorithm. Composite scores were calculated for ADI-R and ADOS-2 (Gotham et al., 2009; Hus and Lord, 2013).
[a]Chi-Square test.
[b]Missing one score.

individual with a neutral expression or a different outdoor scene) (Figure 1). The face stimuli were obtained from the NimStim Face Stimulus Set (http://www.macbrain.org/resources.htm; Tottenham *et al.*, 2009) a validated publicly available set of face stimuli. The scene stimuli were obtained from the 'Open Country' database of photos provided by the Computational Visual Cognition Laboratory (http://cvcl.mit.edu/database.htm).

To ensure engagement with the task, participants were asked to press a button on a handheld response box with their right index finger in response to all standard stimuli, and to press an adjacent button with their right middle finger in response to the deviant stimuli.

## Structural MRI

For each subject, a high resolution $T_1$-weighted spoiled grass gradient recalled inversion recovery 3D MRI sequence was acquired with the following parameters: TI = 300 ms; TR = 8.4 ms; TE = 1.8 ms; flip angle = 15°; 22 cm field of view; 132 slices in coronal plane; 256 × 192 matrix; number of excitations = 2, acquired resolution = 1.5 × 0.9 × 1.1 mm.

## fMRI data pre-processing

A linear shim correction was applied separately for each slice during reconstruction using a magnetic field map acquired automatically by the pulse sequence at the beginning of the scan. fMRI data were then analyzed using SPM8 analysis software (http://www.fil.ion.ucl.ac.uk/spm). Images were realigned to correct for motion, corrected for errors in slice-timing, spatially transformed to standard stereotaxic space [based on the Montreal Neurologic Institute (MNI) coordinate system], resampled every 2 mm using sinc interpolation and smoothed with a 6 mm full-width half-maximum Gaussian kernel to increase the signal-to-noise ratio prior to statistical analysis. Translational movement in millimeters (*x*, *y* and *z*) and rotational motion in degrees (pitch, roll and yaw) were calculated based on the SPM parameters for motion correction of the functional images in each subject. All runs during which motion >6 mm or degrees was observed were excluded from analysis. All subjects who had at least one face run and at least one scene
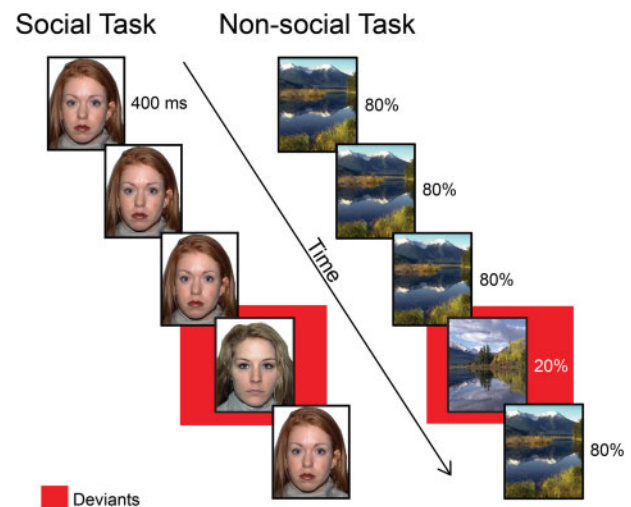


**Fig. 1.** Experimental design: social and non-social attention task. Participants viewed a series of faces (social task) or scenes (non-social task) presented for 400 ms each. On 80% of trials, a 'standard' stimulus was presented. On the remaining 20% of trials, a 'deviant' stimulus was presented.

run below the motion cutoff were included in the analyses. This resulted in 20 TD and 14 ASD participants with all four runs, and six ASD participants with only one face and one scene run. In order to match the groups for number of runs, six TD children from the pool of 20 were matched one-to-one on age, gender and FSIQ to the six ASD participants with only one face and one scene run. For the six matched TD children, only the first scan of each category (i.e. face or scene) was included in the analyses, resulting in 20 participants in each group. There were no group differences in the amount of head motion in the remaining runs (Supplementary Table S1).

## fMRI data analysis: general linear model

Statistical analyses were conducted using the general linear model (GLM) implemented in SPM8. A within-subjects procedure was used to model brain activations related to the

deviant stimuli. Consistent with our previous work (Chen *et al.*, 2015), only brain activation related to deviant stimuli was modeled, while the standard stimuli, which are not explicitly modeled, served as baseline. All contrasts used in this study are based on the comparison of deviant *vs* standard stimuli.

Brain responses were estimated using boxcar functions convolved with a canonical hemodynamic response function (HRF) and a temporal dispersion derivative to account for voxelwise latency differences in hemodynamic response. For each participant, the GLM included regressors of interest modeling the onset times of deviant stimuli and nuisance regressors for head motion to generate the following contrast images: (i) Faces: (Face deviants > Face standards); (ii) Scenes: (Scene deviants > Scene standards) and (iii) Faces *vs* Scenes [(Face deviants > Face standards) *vs* (Scene deviants > Scene standards)]. Given our goal of contrasting differential attentional responses to social *vs* non-social stimuli, the third contrast was the primary focus of our study. These contrast images were entered into an analysis of variance (ANOVA) with group as a between-subjects factor and then used to determine voxelwise group *t* statistics. Significant clusters of activation were determined within the gray matter using a voxelwise height threshold of $P < 0.01$, corrected for multiple comparisons at $P < 0.01$ with a cluster extent of 128 voxels, determined using Monte Carlo simulations (Nichols and Hayasaka, 2003).

### fMRI data analysis: multivariate pattern analysis

Multivariate pattern analysis (MVPA) (Kriegeskorte *et al.*, 2006; Abrams *et al.*, 2011; Cho *et al.*, 2011) was used to identify brain regions that discriminate spatial activation patterns to face *vs* scene deviant stimuli between children with ASD and TD children. The MVPA analysis used a support-vector machine (SVM) classifier with a linear kernel. The activation *t*-map contrasting deviant faces and scenes from the SPM analysis was used as data input to the classifier. As in previous work (Iuculano *et al.*, 2014), at each voxel $v_i$, a $3 \times 3 \times 3$ neighborhood (searchlight) centered at $v_i$ was defined. Therefore, the spatial pattern of voxels in this neighborhood was defined by a 27-dimentional vector. SVM classification was performed using LIBSVM software (http://www.csie.ntu.edu.tw/~cjlin/libsvm). When training the linear SVM classifier, we used a soft-margin approach, setting the regularization parameter C equal to the default parameter of 1, in order to avoid overfitting the data. At each voxel, a Leave-One-Out Cross Validation procedure was used to measure the performance of the classifier in distinguishing children with ASD from TD children during deviant stimuli processing. Data from one subject were left out at a time, to be used as the 'test set' whereas data from the remaining subjects were used as the 'training set', to train the classifier. The class label estimated by the classifier on the test set was compared against the true class. This process was repeated such that every observation was used once for testing purposes. The ratio of correctly estimated class labels to the total number of observations, hereafter referred to as classification accuracy (CA), was then computed. The resulting 3D map of CA at every voxel was used to identify brain regions that distinguish between the groups during deviant stimulus processing. Under the null hypothesis that there is no difference between the two groups, the CAs were assumed to follow the binomial distribution B (*N*, *P*) with parameters *N* equal to the total number of participants in the two groups and *P* equal to 0.5, assuming that under the null hypothesis, the probability of each

group is equal. The CAs were then converted to *P*-values using the binomial distribution. The significant multivariate patterns were determined using a voxel-wise height threshold of $P < 0.05$ and an extent threshold of $P < 0.05$ with family wise error correction using a suprathreshold cluster-size of 453 voxels based on Monte-Carlo simulations, similar to the approach used for thresholding univariate activation patterns.

A sensitivity analysis was run with the same parameters as above except for a different searchlight neighborhood value ($5 \times 5 \times 5$ mm) to examine whether changing this parameter would yield different results. Results from this supplementary analyses are depicted in Supplementary Figure S3 and Table S2.

### fMRI data analysis: generalized psychophysiological interaction

We conducted a generalized psychophysiological interaction (gPPI) analysis (McLaren *et al.*, 2012) to examine the functional interaction between a specific region-of-interest (ROI, here, an independently derived right dAI node of the salience network) and the rest of the brain. PPI measures the temporal relation between this seed region and all other brain voxels, while removing sources of potential confounding influences such as task-related effects and common driving inputs on both the seed and target voxels. A seed ROI was defined as a sphere with 8 mm radius centered at coordinates for the dAI (39, 23, −4) derived from previous work (Uddin *et al.*, 2011). The time series from the seed ROI was de-convolved so as to uncover neuronal activity (physiological variable) and multiplied with the task design (psychological variable) to form an interaction term. This interaction term was convolved with an HRF to form the gPPI regressor (Friston *et al.*, 1997). Subject-level contrast images for deviant face *vs* scene stimuli were generated and entered into a group-level statistical analysis in which brain regions showing significant gPPI effects were determined by testing for a positive slope of the gPPI regressor. The significance of the results was assessed in the same way as described in the GLM section above (i.e. voxelwise height threshold of $P < 0.01$ and a cluster extent of 128 voxels). To examine the relationship between task-based functional connectivity of the dAI and autism symptom severity in children with ASD, we entered the composite score from the ADI-R 'current' algorithm (Hus and Lord, 2013) as a covariate in the analysis. The resulting statistical map was thresholded in the same way as stated above. An exploratory analysis was conducted to investigate the whole-brain task-based connectivity of the vAI between groups (see Supplementary Materials and Figure S4).

## Results

### In-scanner behavioral performance

Behavioral performance on the fMRI task is shown in Figure 2. We conducted a $2 \times 2 \times 2$ repeated measures ANOVA separately for accuracy (i.e. percent correct) and reaction time (i.e. the group average of each subject's median latency, in milliseconds), with Stimulus category (Face, Scene) and Stimulus type (Standard, Deviant) as within-subjects factors and Group (ASD, TD) as a between-subjects factor. The accuracy analysis revealed a main effect of Stimulus type, $F_{(1,33)} = 41.42$, $P < 0.001$, and an interaction between Group × Stimulus category × Stimulus type, $F_{(1,33)} = 5.51$, $P = 0.03$ (Table 2).
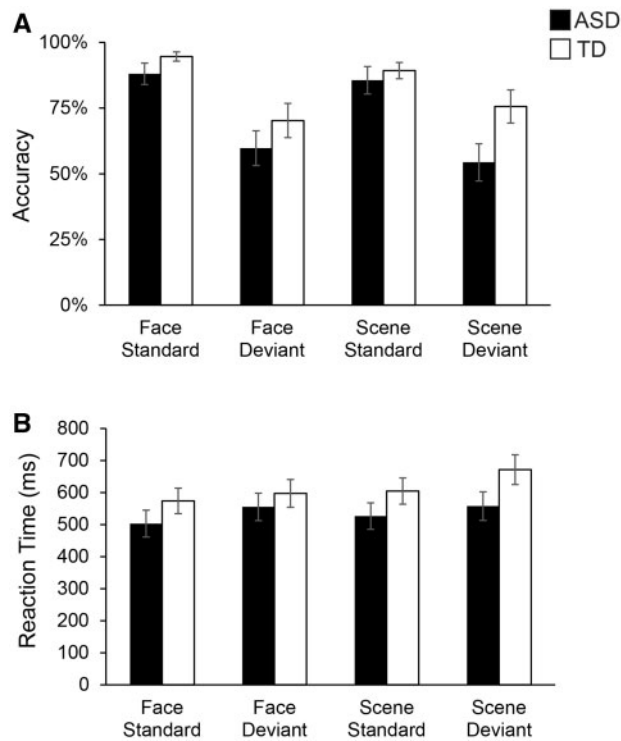
**Fig. 2.** Behavioral performance in ASD and TD children on the Faces and Scenes oddball detection task. (A) Average accuracy (i.e. percent correct) for each Group (ASD, TD) and each Condition (Face, Scene and Standard, Deviant) is shown. (B) Average reaction time (ms) is shown for each Group and each Condition.ANOVA results, shown in Table 2, showed no main effect of Group or interaction of Group with Condition. Error bars represent standard errors of the mean. Behavioral performance data missing for three ASD and two TD participants.

**Table 2.** ANOVA—Performance during faces and scenes tasks

Accuracy

| Source | $df_n$ | $df_d$ | F | P |
|---|---|---|---|---|
| **Group** | 1 | 33 | 3.44 | 0.07 |
| **Stimulus Category (Faces, Scenes)** | 1 | 33 | 0.40 | 0.53 |
| **Stimulus Type (Standard, Deviant)** | 1 | 33 | 41.42 | <0.001** |
| **Group × Stim. Category** | 1 | 33 | 0.42 | 0.52 |
| **Group × Stim. Type** | 1 | 33 | 2.04 | 0.16 |
| **Stim. Category × Stim. Type** | 1 | 33 | 1.96 | 0.17 |
| **Group × Stim. Category × Stim. Type** | 1 | 33 | 5.51 | 0.03 |

Reaction Time

| Source | $df_n$ | $df_d$ | F | P |
|---|---|---|---|---|
| **Group** | 1 | 33 | 1.75 | 0.19 |
| **Stimulus Category (Faces, Scenes)** | 1 | 33 | 5.16 | 0.03 |
| **Stimulus Type (Standard, Deviant)** | 1 | 33 | 19.39 | <0.001** |
| **Group × Stim. Category** | 1 | 33 | 1.80 | 0.19 |
| **Group × Stim. Type** | 1 | 33 | 0.03 | 0.86 |
| **Stim. Category × Stim. Type** | 1 | 33 | 0.95 | 0.34 |
| **Group × Stim. Category × Stim. Type** | 1 | 33 | 6.75 | 0.01 |

Results of $2 \times 2 \times 2$ repeated-Measures ANOVA with one between-subjects factor (Group) and two within-subject factors (Stimulus Category and Stimulus Type). **$P < 0.001$, after correction (see text).

Analysis of reaction time revealed a main effect of Stimulus category, $F(1,33) = 5.16$, $P = 0.03$, main effect of Stimulus type, $F(1,33) = 19.39$, $P < 0.001$, and a Group × Stimulus category × Stimulus type interaction, $F(1,33) = 6.75$, $P = 0.01$ (Table 2). Crucially, there was no main effect of Group, and no interaction of Group with Stimulus category or with Stimulus type individually. Using Bonferroni correction for multiple comparisons, only the main effect of Stimulus type remained significant for both accuracy and reaction time analyses. Finally, within the ASD group, accuracy in the Face deviant condition was significantly negatively correlated with ASD symptom severity as assessed using the ADI-R composite score ($r = -0.55$; $P = 0.03$).

Successful discrimination of the standard and deviant stimuli was measured using d-prime, a sensitivity index for signal detection, computed by subtracting the z-transformed false alarm rate (i.e. incorrectly identified standard stimulus) from the z-transformed hit rate (i.e. correctly identified deviant stimulus): $d' = z(H)–z(F)$. We found a trend for lower d-prime scores in the ASD group ($P < 0.10$ for faces and $P < 0.07$ for scenes) but there was no significant interaction between Group and Stimulus type, $F(1,32) = 0.04$, $P < 0.85$ (Supplementary Figure S1).

### Brain activation to deviant faces and scenes in the ASD and TD groups

We first examined fMRI responses within each group to deviant stimuli in the face and scene oddball tasks. We found that there was a large degree of overlap in activation profiles for both tasks between the TD children and children with ASD. For the social attention task, both groups of children showed greater activation to deviant faces in the anterior insula and anterior cingulate cortex nodes of the salience network (Figure 3A). Overlapping insula activation to face deviants in both ASD and TD groups was localized to the dAI subdivision, as demarcated by parcellation of resting-state fMRI (Deen *et al.*, 2011). Both groups also showed activation in the lateral occipital gyrus (LOC), angular gyrus, supramarginal gyrus, precuneus cortex and fusiform gyrus (FG). During the non-social oddball task, both groups showed greater activation to deviant scenes in the bilateral FG (Figure 3B).

We next examined fMRI responses to deviant faces compared with deviant scenes within each group. Children with ASD showed greater activation to deviant faces in the right dAI and vAI, and greater activation to deviant scenes in the left FG, left parahippocampal gyrus, left lingual gyrus and right LOC (Supplementary Figure S2). TD children did not show differential activation to faces *vs* scenes in any brain region.

### Group differences in brain activation to deviant faces *vs* scenes

We then directly compared brain responses to deviant faces *vs* scenes between the ASD and TD groups. No group differences in activation were detected at a threshold of $P < 0.01$, corrected for multiple comparisons. Based on our *a priori* hypotheses with respect to insula dysfunction in ASD, we then probed group differences using a threshold of $P < 0.05$, cluster-corrected at $P < 0.01$, with a 562 voxel extent. We found that, in contrast to their TD peers, children with ASD displayed greater activation of the right insula when viewing deviant faces *vs* scenes (Figure 4). Based on previously published parcellation maps (Deen *et al.*,
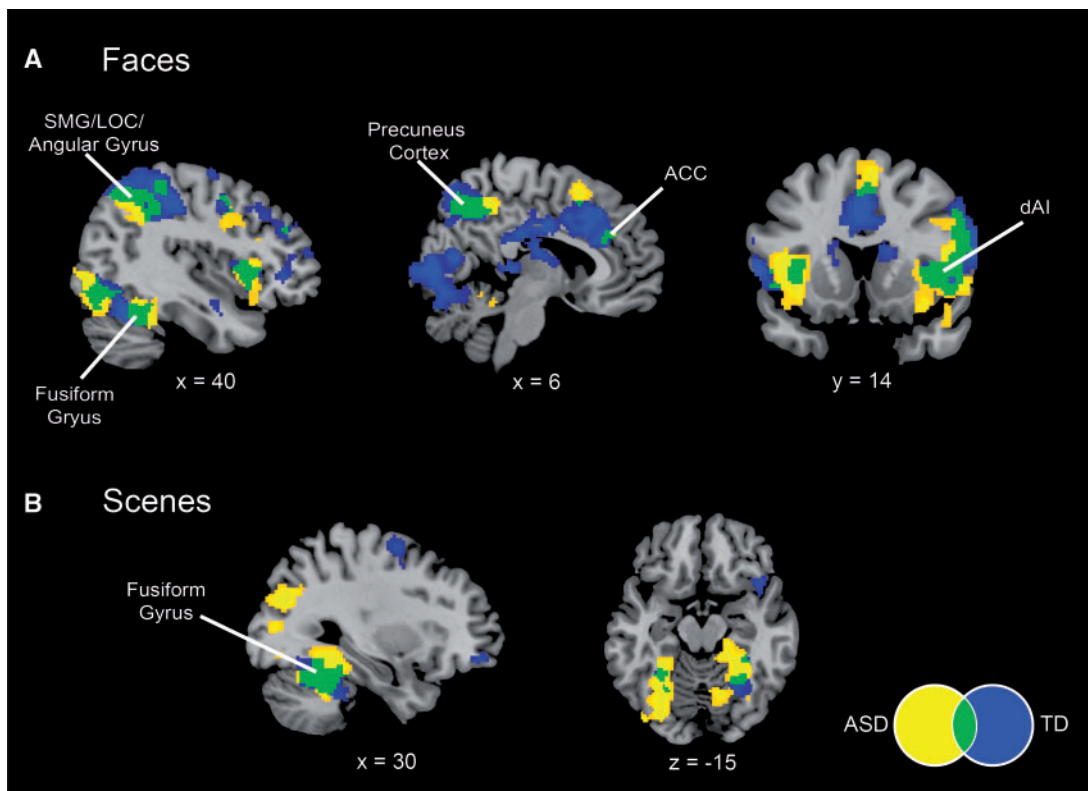
**Fig. 3.** Differential activation to deviant faces and scenes. (A) Activation to Faces (deviants > standards) in children with autism spectrum disorder (ASD, yellow) and typically-developing (TD) children (blue), showing overlap (green) in bilateral dAI, anterior cingulate cortex (ACC), supramarginal gyrus (SMG), lateral occipital cortex (LOC), angular gyrus, fusiform gyrus and precuneus cortex. (B) Activation to Scenes (deviants > standards) in children with ASD and TD children. Both groups show activation in the fusiform gyrus. All images thresholded at P < 0.01 and 128 voxel extent.

2011), these differences were localized to the ventral anterior subdivision of the insula (Figure 5).

## Group differences in multivariate activation patterns associated with deviant faces *vs* scenes

To further investigate differences in neural organization for social *vs* non-social attention tasks, we compared the patterns of activation in children with ASD *vs* TD children using an MVPA. This analysis highlighted several cortical regions where activity patterns could reliably classify children with ASD and their TD peers. Notably, high cross-validation classification accuracies (70–90%) were found in the insula and temporal pole (Figure 6 and Table 3). The insula cluster showed prominent overlap with the dorsal anterior subdivision (Figure 5). This result indicates that despite similar levels of activation, children with ASD engage the right dAI differently from their TD peers. Results for the sensitivity analysis using an alternate neighborhood size are shown in Supplementary Materials (Supplementary Figure S3 and Table S2).

## Group differences in dAI connectivity associated with processing deviant faces *vs* scenes

Next, we used gPPI analysis to investigate group differences in functional connectivity of the dAI to deviant faces *vs* scenes. Compared with TD children, the ASD group showed reduced dAI connectivity with motor, sensory and visual processing regions, including bilateral pre- and post-central gyri, supplementary motor area, middle frontal gyrus, middle and superior temporal gyri and right lateral occipital cortex (Figure 7).

In contrast, the ASD group showed greater connectivity between the right and left dAI while processing face compared with scene deviant events. These results suggest that network interactions within the salience network are stronger in ASD, whereas interactions between the salience network and other brain systems are weaker in this population, compared with TD children.

Based on the group differences in activation in the vAI, we also conducted an exploratory analysis of task-based connectivity of this region to the rest of the brain. We found that TD children exhibited significantly greater connectivity of the vAI with the bilateral frontal pole than children with ASD when viewing deviant faces *vs* scenes (Supplementary Figure S4).

## Relation between ASD symptom severity and activation to deviant faces *vs* scenes

Within the ASD group, current symptom severity, assessed using a composite ADI-R index, was associated with greater activation in the right posterior insula and right parahippocampal gyrus (Supplementary Figure S5). This result suggests that multiple subdivisions of the right insula are functionally aberrant in children with ASD.

## Relation between ASD symptom severity and dAI connectivity

gPPI analysis was used to determine the relation between ASD symptom severity and dAI connectivity during the processing of deviant faces *vs* scenes. In children with ASD, right dAI connectivity with middle temporal and angular gyri as well as
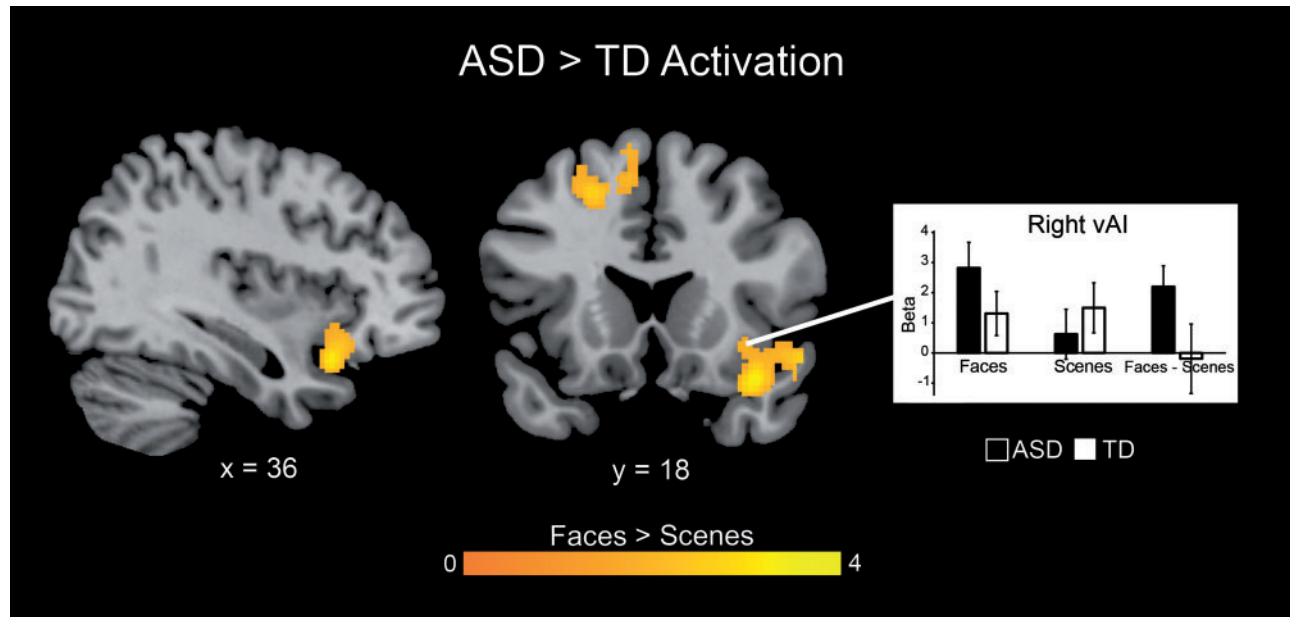
**Fig. 4.** Group differences in brain activation to deviant Faces *vs* Scenes. Children with ASD exhibited significantly greater activity than TD children in the right vAI, and in the superior and middle frontal gyri when viewing deviant faces *vs* scenes. Images thresholded at $P < 0.05$ and 562 voxel extent, color bar indicates *t*-score. Graph shows activation levels in each group. No brain regions showed higher activation in TD children compared to children with ASD.
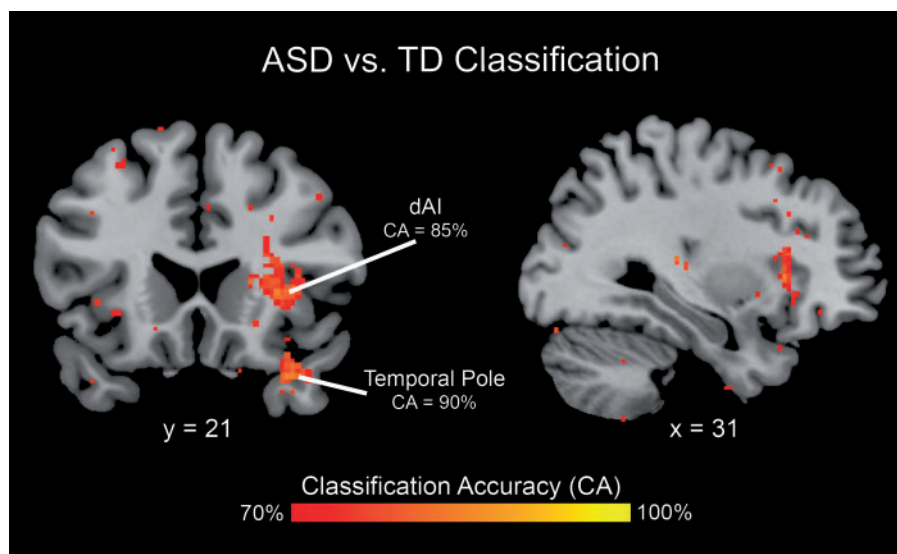


**Fig. 5.** Multivariate brain activity patterns distinguish children with ASD from TD children. Multivariate analysis revealed significant differences in spatial activation patterns between children with ASD and TD children in the dAI (with a classification accuracy peak of 85%) and in the temporal pole (with a classification accuracy peak of 90%). Brain activation patterns associated with processing deviant faces vs scenes were used as data input to the classifier.

lingual and parahippocampal gyri was modulated by ASD symptom severity, as measured by the ADI-R composite score. Specifically, children with ASD who exhibited lower social impairments showed increased connectivity during face processing (Figure 8). This result suggests that higher dAI connectivity with temporo-parietal regions during processing of social *vs* non-social stimuli may facilitate social functioning in ASD.

## Discussion

Reduced attention to social stimuli is a hallmark of ASD. Yet, the brain systems mediating attention to salient social information in young children with ASD are relatively unknown. A salience network with key nodes in the anterior insula and anterior cingulate cortex is thought to underlie neural responses to meaningful stimuli (Seeley *et al.*, 2007). The dAI node, in particular, integrates salient information from the external world to coordinate dynamic interactions between the salience network and other large-scale brain networks (Menon and Uddin, 2010; Uddin, 2015). We have recently demonstrated intrinsic functional hyperconnectivity of the salience network in children with ASD, and suggested that this increased within-network connectivity could hinder between-network interactions necessary for flexible and adaptive behavior (Uddin
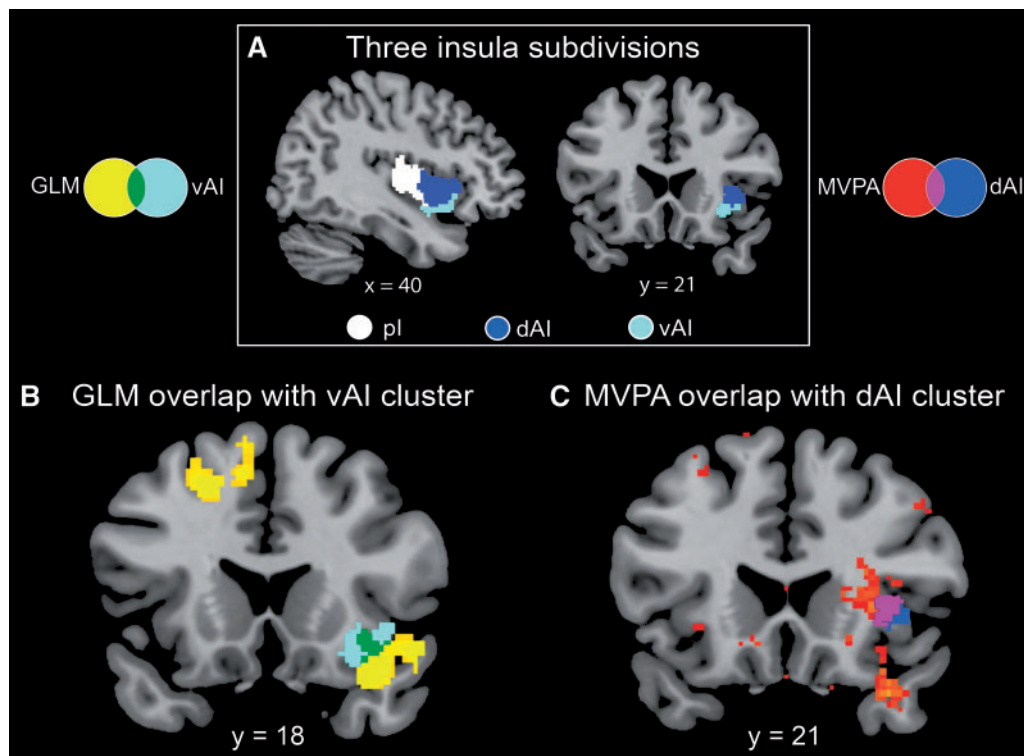
**Fig. 6.** Group differences in activation and multivariate patterns within insular subdivisions. (A) The three subdivisions of the insula as identified by cluster analysis (Deen et al., 2011) include the posterior insula (pI; white), the dorsal anterior insula (dAI; blue) and the ventral anterior insula (vAI; cyan). (B) Results from the univariate analysis of group differences in activation elicited by deviant faces vs scenes (Figure 3) showed overlap (green) with the vAI cluster. (C) Multivariate analysis of group differences in activation patterns elicited by deviant faces vs scenes (Figure 4) revealed prominent overlap (purple) with the dAI cluster.

**Table 3.** Brain areas that showed significant differences in multivariate activation patterns between ASD and TD groups during deviant face *vs* scene processing

| Region | Cluster size (voxels) | Peak CA (%) | MNI coordinates | | |
|---|---|---|---|---|---|
| | | | x | y | z |
| R dorsal anterior insula | 132 | 85 | 34 | 22 | 4 |
| R temporal pole | 86 | 90 | 34 | 18 | −28 |

CA, classification accuracy

*et al.*, 2013a). Functional connectivity of portions of the insula has previously been linked to severity of autism traits in neurotypical adults (Di Martino *et al.*, 2009b). Results from mining a large dataset also point to altered functional connectivity patterns of the mid- and posterior insula in individuals with ASD (Di Martino *et al.*, 2014).

In this work, we use a classic oddball detection paradigm to investigate the activation and functional connectivity profile of the salience network in children with ASD. Our task was a simplified oddball paradigm chosen to be developmentally appropriate and easy to perform for young children. Analysis of behavioral performance during the task indicated that there was no main effect of Group in either accuracy or reaction time, and Group did not interact with Stimulus category (Faces, Scenes) nor with Stimulus type (Standard, Deviant) (Figure 2 and Table 2). There was a significant Group × Stimulus type × Stimulus category interaction for accuracy and reaction time, suggesting that children with ASD were specifically less accurate when processing

scene deviants than the TD group, while all other factors were comparable across the two groups. After corrections for multiple comparisons, we found that children with ASD and TD children showed similar patterns of behavioral responses on both accuracy and reaction time in response to social as well as non-social stimuli, as expected for a relatively simple task. We also examined d-prime, a measure of sensitivity, in this case, a participants' ability to discriminate standard from deviant stimuli. Children with ASD showed a trend for lower d-prime scores (Supplementary Figure S5) but there was no significant interaction between Group and Stimulus type. Because the task was simplified in order to be developmentally appropriate, it was expected that high-functioning children with ASD would perform comparably to their TD peers. Our findings are consistent with previous behavioral studies in young children, which have found that high-functioning children with ASD do not differ from TD peers in attentional disengagement and social orienting (Fischer *et al.*, 2014) and the majority of neuroimaging studies of ASD (Nomi and Uddin, 2015b).

We observed that children with ASD engaged different brain systems to reach a similar level of behavioral performance as their TD peers. In line with previous research in adults with ASD (Dichter *et al.*, 2009; Sabatino *et al.*, 2013), we find that children with ASD also show greater activation than TD children in the right anterior insula during processing of social (face) compared with non-social (scene) deviants. Although we had predicted that the most prominent activation differences would be observed in the dAI subdivision, which is involved in attention to salient stimuli and causally switching between brain networks and states, we found no group differences in overall
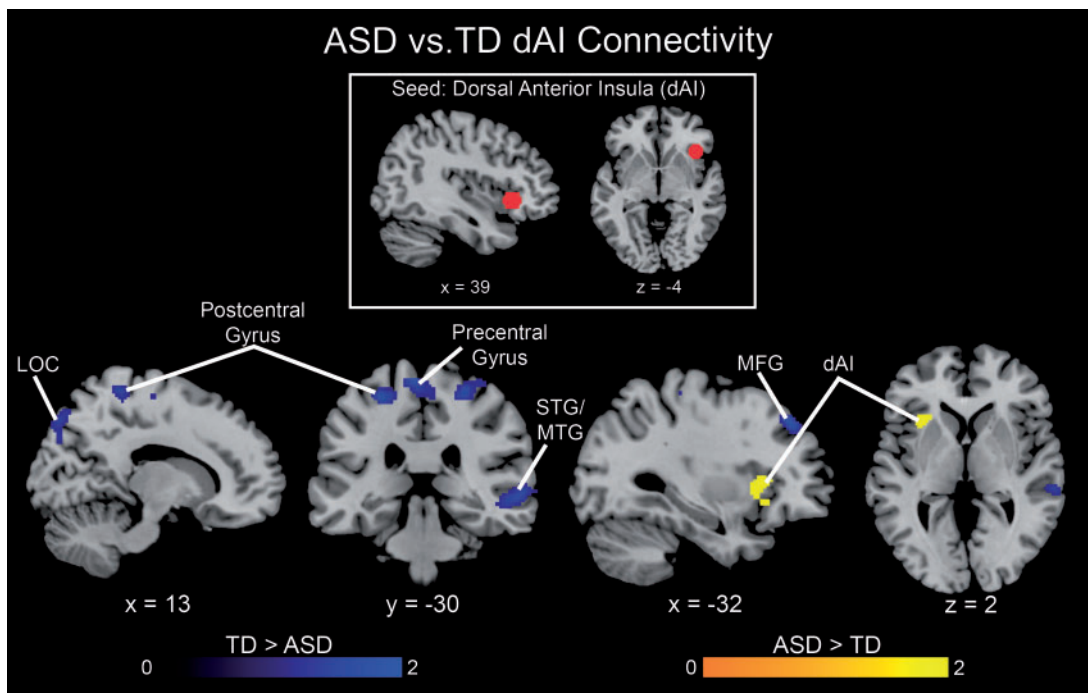
**Fig. 7.** Group differences in dAI connectivity. Functional connectivity associated with deviant face *vs* scene processing was examined using a gPPI analysis with a right dAI seed (MNI coordinates: 39, 23, −4). The ASD group showed greater connectivity (yellow) within the salience network, i.e. between the right dAI seed and left dAI. In contrast, the TD group showed greater connectivity (blue) across networks, i.e. between the dAI seed and right LOC, bilateral pre- and post-central gyri, as well as right superior and middle temporal gyri. All images thresholded at $P < 0.01$ and 128 voxel extent, color bar indicates *t*-score.
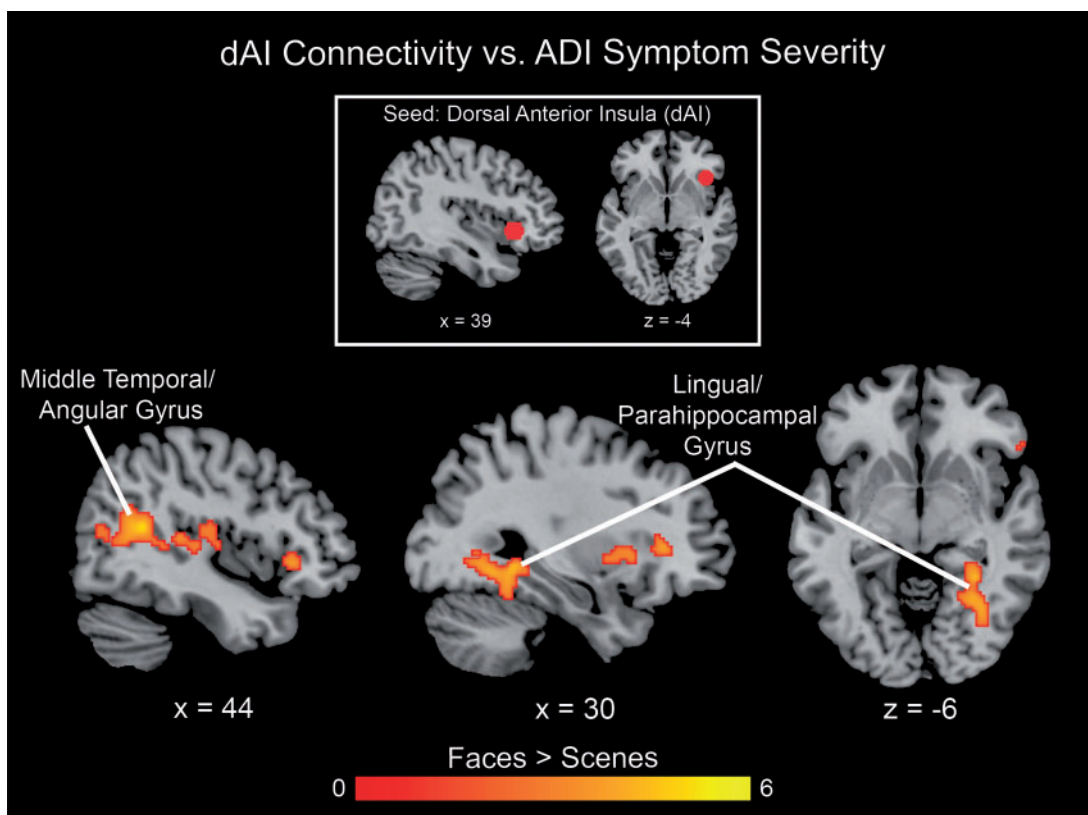


**Fig. 8.** dAI connectivity correlated with symptom severity in ASD. gPPI analysis with a right dAI seed (MNI coordinates: 39, 23, −4) revealed that connectivity of this seed with middle temporal and angular gyri as well as lingual and parahippocampal gyri were negatively correlated with autism symptom severity, as measured by the ADI-R composite score. All images thresholded at $P < 0.01$ and 128 voxel extent, color bar indicates *t*-score.

activation levels in that region. Instead, we found robust activation differences in the vAI subdivision of the insula. Meta-analytic decoding analyses suggest that the vAI is consistently involved in affective and socio-emotional processing (Chang *et al.*, 2013; Uddin *et al.*, 2014a), and is functionally co-active with limbic regions including cingulate cortex, orbitofrontal cortices and temporal poles (Uddin *et al.*, 2014a). The current findings suggest that children with ASD may be hyper-reactive to social deviant stimuli in regions of the brain important for processing emotional relevance. This enhanced vAI activation in children with ASD during social target detection may reflect heightened emotional reactivity in children with the disorder (Skokauskas and Gallagher, 2010).

Crucially, we also found that the BOLD signal from the dAI, while not differing in magnitude between groups, exhibited spatial activation patterns that were sufficient to reliably discriminate children with ASD from TD children. This region is activated across most task domains that have been investigated, and has been posited to play a role in functional integration between different brain systems (Kurth *et al.*, 2010). The dAI is one of the most 'diverse' (Uddin *et al.*, 2014a) and 'flexible' (Yeo *et al.*, 2015) brain regions, further supporting its role in binding or integration across multiple brain systems. This region is consistently involved in higher-level cognitive processes including inhibition, error processing, conflict resolution and switching (Zimmerman *et al.*, 2012), and plays a role in coordinating brain network dynamics in children (Uddin *et al.*, 2011, 2014b) and adults (Sridharan *et al.*, 2008; Cai *et al.*, 2014).

These findings suggest that the atypical responses of the dAI to social stimuli may contribute to difficulties with social attention that are characteristic of the disorder. This finding also highlights the utility of multivariate approaches for revealing subtle differences in brain organization in clinical populations. While the magnitude of dAI activation is indistinguishable between the groups, the multivariate findings suggest that the differences in functional integrity observed within this region may take a different form than those observed in the vAI. One possibility is that high-level integration and executive function is differentially implemented by the dAI in children with ASD and TD children. Taken together, the current results suggest that the anterior insula is a major locus of dysfunction in ASD, in which a combination of affective hyper-responsivity in the vAI combined with altered dAI organization and functional connectivity contribute to social attention difficulties observed in children with ASD.

The only previous fMRI study of social attention in children with ASD used a social orienting paradigm, measuring neural responses to spatial cueing with social (eye gaze) and non-social (arrows) stimuli. Greene *et al.* (2011) report hypo-activity in fronto-parietal networks in children with ASD during social cueing. While that study did not examine insula responses directly, they did report greater activation in the dAI for the TD group during viewing of social *vs* non-social cues. A study of adults with ASD reported increased activation to social deviants in the right vAI (Sabatino *et al.*, 2013). These reports suggest that characterizing functional abnormalities within specific insular subdivisions could lead to greater clarity in understanding the neural basis of social attention deficits in autism (Uddin, 2015).

We previously demonstrated increased within-network connectivity in the salience network in children with ASD, and suggested that this hyperconnectivity within the network could prevent flexibility in switching between brain networks (Uddin *et al.*, 2013a). Consistent with this prediction, we found increased right to left dAI connectivity in children with ASD in the present study. In contrast, children with ASD showed decreased connectivity with multiple brain regions involved in processing deviant stimuli, and more severely affected children with ASD exhibited greater hypo-connectivity. Taken together, these results suggest that network interactions within the salience network are stronger in ASD, whereas interactions between the salience network and other brain systems are weaker in this population in this behavioral context.

An emerging literature suggests developmentally dependent alterations of functional connectivity in ASD (Uddin *et al.*, 2013b; Nomi and Uddin, 2015a), challenging earlier general under-connectivity accounts (Just *et al.*, 2012). The current results are compatible with the hypothesis that functional hyperconnectivity detected using intrinsic fMRI (Di Martino *et al.*, 2011; Keown *et al.*, 2013; Supekar *et al.*, 2013) may result in brain network configurations that are less flexible during task states, especially during processing of socially demanding stimuli such as faces.

## Acknowledgements

## Funding

## Supplementary data

Supplementary data are available at *SCAN* online.

## Conflict of interest.

None declared.

## References

Abrams, D.A., Bhatara, A., Ryali, S., Balaban, E., Levitin, D.J., Menon, V. (2011). Decoding temporal structure in music and speech relies on shared brain resources but elicits different fine-scale spatial patterns. *Cerebral Cortex*, **21**(7), 1507–18.

Ardekani, B.A., Choi, S.J., Hossein-Zadeh, G.A., Porjesz, B., Tanabe, J.L., Lim, K.O., et al. (2002). Functional magnetic resonance imaging of brain activity in the visual oddball task. *Brain Research Cognitive Brain Research*, **14**(3), 347–56.

Cai, W., Chen, T., Ryali, S., Kochalka, J., Li, C.S., Menon, V. (2015). Causal interactions within a frontal-cingulate-parietal network during cognitive control: convergent evidence from a multisite-multitask investigation. *Cerebral Cortex*. doi: 10.1093/cercor/bhv046.

Cai, W., Ryali, S., Chen, T., Li, C.S., Menon, V. (2014). Dissociable roles of right inferior frontal cortex and anterior insula in inhibitory control: evidence from intrinsic and task-related functional parcellation, connectivity, and response profile analyses across multiple datasets. *Journal of Neuroscience*, **34**(44), 14652–67.

Chang, L.J., Yarkoni, T., Khaw, M.W., Sanfey, A.G. (2013). Decoding the role of the insula in human cognition: functional parcellation and large-scale reverse inference. *Cerebral Cortex*, **23**(3), 739–49.

Chen, T., Michels, L., Supekar, K., Kochalka, J., Ryali, S., Menon, V. (2015). Role of the anterior insular cortex in integrative causal signaling during multisensory auditory-visual attention. *The European Journal of Neuroscience*, **41**(2), 264–74.

Chevallier, C., Kohls, G., Troiani, V., Brodkin, E.S., Schultz, R.T. (2012). The social motivation theory of autism. *Trends in Cognitive Sciences*, **16**(4), 231–9.

Cho, S., Ryali, S., Geary, D.C., Menon, V. (2011). How does a child solve 7 + 8? Decoding brain activity patterns associated with counting and retrieval strategies. *Developmental Science*, **14**(5), 989–1001.

Crottaz-Herbette, S., Lau, K.M., Glover, G.H., Menon, V. (2005). Hippocampal involvement in detection of deviant auditory and visual stimuli. *Hippocampus*, **15**(1), 132–9.

Crottaz-Herbette, S., Menon, V. (2006). Where and when the anterior cingulate cortex modulates attentional response: combined fMRI and ERP evidence. *Journal of Cognitive Neuroscience*, **18**(5), 766–80.

Dawson, G., Toth, K., Abbott, R., Osterling, J., Munson, J., Estes, A., *et al.* (2004). Early social attention impairments in autism: social orienting, joint attention, and attention to distress. *Developmental Psychology*, **40**(2), 271–83.

Deen, B., Pitskel, N.B., Pelphrey, K.A. (2011). Three systems of insular functional connectivity identified with cluster analysis. *Cerebral Cortex*, **21**(7), 1498–506.

Di Martino, A., Kelly, C., Grzadzinski, R., Zuo, X.N., Mennes, M., Mairena, M.A., *et al.* (2011). Aberrant striatal functional connectivity in children with autism. *Biological Psychiatry*, **69**(9), 847–56.

Di Martino, A., Ross, K., Uddin, L.Q., Sklar, A.B., Castellanos, F.X., Milham, M.P. (2009a). Functional brain correlates of social and nonsocial processes in autism spectrum disorders: an activation likelihood estimation meta-analysis. *Biological Psychiatry*, **65**(1), 63–74.

Di Martino, A., Shehzad, Z., Kelly, C., Roy, A.K., Gee, D.G., Uddin, L.Q., *et al.* (2009b). Relationship between cingulo-insular functional connectivity and autistic traits in neurotypical adults. *The American Journal of Psychiatry*, **166**(8), 891–9.

Di Martino, A., Yan, C.G., Li, Q., Denio, E., Castellanos, F.X., Alaerts, K., *et al.* (2014). The autism brain imaging data exchange: towards a large-scale evaluation of the intrinsic brain architecture in autism. *Molecular Psychiatry*, **19**(6), 659–67.

Dichter, G.S., Felder, J.N., Bodfish, J.W. (2009). Autism is characterized by dorsal anterior cingulate hyperactivation during social target detection. *Social Cognitive and Affective Neuroscience*, **4**(3), 215–26.

Dickstein, D.P., Pescosolido, M.F., Reidy, B.L., Galvan, T., Kim, K.L., Seymour, K.E., *et al.* (2013). Developmental meta-analysis of the functional neural correlates of autism spectrum disorders. *Journal of the American Academy of Child and Adolescent Psychiatry*, **52**(3), 279–89. e216.

Downar, J., Crawley, A.P., Mikulis, D.J., Davis, K.D. (2000). A multimodal cortical network for the detection of changes in the sensory environment. *Nature Neuroscience*, **3**(3), 277–83.

Fischer, J., Koldewyn, K., Jiang, Y.V., Kanwisher, N. (2014). Unimpaired attentional disengagement and social orienting in children with autism. *Clinical Psychological Science*, **2**, 214–23.

Friston, K.J., Buechel, C., Fink, G.R., Morris, J., Rolls, E., Dolan, R.J. (1997). Psychophysiological and modulatory interactions in neuroimaging. *Neuroimage*, **6**(3), 218–29.

Gotham, K., Pickles, A., Lord, C. (2009). Standardizing ADOS scores for a measure of severity in autism spectrum disorders. *Journal of Autism and Developmental Disorders*, **39**(5), 693–705.

Gotham, K., Risi, S., Pickles, A., Lord, C. (2007). The autism diagnostic observation schedule: revised algorithms for improved diagnostic validity. *Journal of Autism and Developmental Disorders*, **37**(4), 613–27.

Greene, D.J., Colich, N., Iacoboni, M., Zaidel, E., Bookheimer, S.Y., Dapretto, M. (2011). Atypical neural networks for social orienting in autism spectrum disorders. *Neuroimage*, **56**(1), 354–62.

Hus, V., Lord, C. (2013). Effects of child characteristics on the Autism Diagnostic Interview-Revised: implications for use of scores as a measure of ASD severity. *Journal of Autism and Developmental Disorders*, **43**(2), 371–81.

Iuculano, T., Rosenberg-Lee, M., Supekar, K., Lynch, C.J., Khouzam, A., Phillips, J., *et al.* (2014). Brain organization underlying superior mathematical abilities in children with autism. *Biological Psychiatry*, **75**(3), 223–30.

Just, M.A., Keller, T.A., Malave, V.L., Kana, R.K., Varma, S. (2012). Autism as a neural systems disorder: a theory of frontal-posterior underconnectivity. *Neuroscience and Biobehavioral Reviews*, **36**(4), 1292–313.

Kanner, L. (1943). Autistic disturbances of affective contact. *Nervous Child*, **22**, 217–50.

Keown, C.L., Shih, P., Nair, A., Peterson, N., Mulvey, M. E., Muller, R.A. (2013). Local functional overconnectivity in posterior brain regions is associated with symptom severity in autism spectrum disorders. *Cell Reports*, **5**(3), 567–52.

Kim, H. (2014). Involvement of the dorsal and ventral attention networks in oddball stimulus processing: a meta-analysis. *Human Brain Mapping*., **5**(5), 2265–84.

Kriegeskorte, N., Goebel, R., Bandettini, P. (2006). Information-based functional brain mapping. *Proceedings of the National Academy of Sciences of the United States of America*, **103**(10), 3863–8.

Kurth, F., Zilles, K., Fox, P.T., Laird, A.R., Eickhoff, S.B. (2010). A link between the systems: functional differentiation and integration within the human insula revealed by meta-analysis. *Brain Structure and Function*, **214**(5-6), 519–34.

Lord, C., Risi, S., Lambrecht, L., Cook, E.H., Jr, Leventhal, B.L., DiLavore, P.C., *et al.* (2000). The autism diagnostic observation schedule-generic: a standard measure of social and communication deficits associated with the spectrum of autism. *Journal of Autism and Developmental Disorders*, **30**(3), 205–23.

Lord, C., Rutter, M. Le Couteur, A. (1994). Autism Diagnostic Interview-Revised: a revised version of a diagnostic interview for caregivers of individuals with possible pervasive developmental disorders. *Journal of Autism and Developmental Disorders*, **24**(5), 659–85.

McLaren, D.G., Ries, M.L., Xu, G. Johnson, S.C. (2012). A generalized form of context-dependent psychophysiological interactions (gPPI): a comparison to standard approaches. *Neuroimage*, **61**(4), 1277–86.

Menon, V. (2015). Salience network. In: Toga, A.W., editor. *Brain Mapping: An Encyclopedic Reference*, **vol. 2**, pp. 597–611. London, UK: Elsevier.

Menon, V. Uddin, L.Q. (2010). Saliency, switching, attention and control: a network model of insula function. *Brain Structure and Function*, **214**(5-6), 655–67.

Nichols, T. Hayasaka, S. (2003). Controlling the familywise error rate in functional neuroimaging: a comparative review. *Statistical Methods in Medical Research*, **12**(5), 419–46.

Nomi, J.S. Uddin, L.Q. (2015a). Developmental changes in large-scale network connectivity in autism. *Neuroimage Clinical*, **7**, 732–41.

Nomi, J.S. Uddin, L.Q. (2015b). Face processing in autism spectrum disorders: from brain regions to brain networks. *Neuropsychologia*, **71**, 201–16.

Sabatino, A., Rittenberg, A., Sasson, N.J., Turner-Brown, L., Bodfish, J.W. Dichter, G.S. (2013). Functional neuroimaging of social and nonsocial cognitive control in autism. *Journal of Autism and Developmental Disorders*, **43**(12), 2903–13.

Scott-Van Zeeland, A.A., Abrahams, B.S., Alvarez-Retuerto, A.I., Sonnenblick, L.I., Rudie, J.D., Ghahremani, D., *et al*. (2010). Altered functional connectivity in frontal lobe circuits is associated with variation in the autism risk gene CNTNAP2. *Science Translational Medicine*, **2**(56), 56ra80.

Seeley, W.W., Menon, V., Schatzberg, A.F., Keller, J., Glover, G.H., Kenna, H., *et al*. (2007). Dissociable intrinsic connectivity networks for salience processing and executive control. *Journal of Neuroscience*, **27**(9), 2349–56.

Skokauskas, N. Gallagher, L. (2010). Psychosis, affective disorders and anxiety in autistic spectrum disorder: prevalence and nosological considerations. *Psychopathology*, **43**(1), 8–16.

Sridharan, D., Levitin, D.J. Menon, V. (2008). A critical role for the right fronto-insular cortex in switching between central-executive and default-mode networks. *Proceedings of the National Academy of Sciences of the United States of America*, **105**(34), 12569–74.

Supekar, K., Uddin, L.Q., Khouzam, A., Phillips, J., Gaillard, W.D., Kenworthy, L.E., *et al*. (2013). Brain hyperconnectivity in children with autism and its links to social deficits. *Cell Reports*, **5**(3), 738–47.

Tottenham, N., Tanaka, J.W., Leon, A.C., McCarry, T., Nurse, M., Hare, T.A., *et al*. (2009). The NimStim set of facial expressions: judgments from untrained research participants. *Psychiatry Research*, **168**(3), 242–9.

Uddin, L.Q. (2015). Salience processing and insular cortical function and dysfunction. *Nature Reviews Neuroscience*, **16**(1), 55–61.

Uddin, L.Q., Kinnison, J., Pessoa, L. Anderson, M.L. (2014a). Beyond the tripartite cognition-emotion-interoception model of the human insular cortex. *Journal of Cognitive Neuroscience*, **26**(1), 16–27.

Uddin, L.Q., Menon, V. (2009). The anterior insula in autism: under-connected and under-examined. *Neuroscience and Biobehavioral Reviews*, **33**(8), 1198–203.

Uddin, L.Q., Supekar, K., Lynch, C.J., Cheng, K.M., Odriozola, P., Barth, M.E., *et al*. (2014b). Brain state differentiation and behavioral inflexibility in autism. *Cerebral Cortex*. doi: 10.1093/cercor/bhu161.

Uddin, L.Q., Supekar, K., Lynch, C.J., Khouzam, A., Phillips, J., Feinstein, C., *et al*. (2013a). Salience network-based classification and prediction of symptom severity in children with autism. *Journal of the American Medical Association Psychiatry*, **70**(8), 869–79.

Uddin, L.Q., Supekar, K. Menon, V. (2013b). Reconceptualizing functional brain connectivity in autism from a developmental perspective. *Frontiers in Human Neuroscience*, **7**, 458.

Uddin, L.Q., Supekar, K.S., Ryali, S. Menon, V. (2011). Dynamic reconfiguration of structural and functional connectivity across core neurocognitive brain networks with development. *Journal of Neuroscience*, **31**(50), 18578–89.

Wechsler, D. (1999). Wechsler Abbreviated Scale of Intelligence. San Antonio, TX: The Psychological Corporation.

Yeo, B.T., Krienen, F.M., Eickhoff, S.B., Yaakub, S.N., Fox, P.T., Bucker, R.L., *et al*. (2015). Functional specialization and flexibility in human association cortex. *Cerebral Cortex*, **25**(10), 3654–72.

Zimmerman, M., Dalrymple, K., Young, D., Chelminski, I. Martinez, J. (2012). An empirical examination of Gunderson's proposed revision of the diagnostic algorithm for borderline personality disorder. *Journal of Personality Disorders*, **26**(6), 880–9.